

PAPER

# Electrical wire explosion process of copper/silver hybrid nano-particle ink and its sintering via flash white light to achieve high electrical conductivity

To cite this article: Wan-Ho Chung *et al* 2016 *Nanotechnology* **27** 205704

View the [article online](#) for updates and enhancements.

## Related content

- [Highly conductive copper nano/microparticles ink via flash light sintering for printed electronics](#)  
Sung-Jun Joo, Hyun-Jun Hwang and Hak-Sung Kim
- [Multi-pulse flash light sintering of bimodal Cu nanoparticle-ink for highly conductive printed Cu electrodes](#)  
Myeong-Hyeon Yu, Sung-Jun Joo and Hak-Sung Kim
- [In situ monitoring of a flash light sintering process using silver nano-ink for producing flexible electronics](#)  
Wan-Ho Chung, Hyun-Jun Hwang, Seung-Hyun Lee et al.

# Electrical wire explosion process of copper/silver hybrid nano-particle ink and its sintering via flash white light to achieve high electrical conductivity

Wan-Ho Chung<sup>1</sup>, Yeon-Taek Hwang<sup>1</sup>, Seung-Hyun Lee<sup>3</sup> and Hak-Sung Kim<sup>1,2</sup>

<sup>1</sup> Department of Mechanical Convergence Engineering, Hanyang University, 17 Haendang-Dong, Seongdong-Gu, Seoul, 133-791, Korea

<sup>2</sup> Institute of Nano Science and Technology, Hanyang University, Seoul, 133-791, Korea

<sup>3</sup> Department of Printed Electronics, Korea Institute of Machinery and Materials 156, Gajungbuk No, Yuseong-Gu, Daejeon, 305-343, Korea

E-mail: [kima@hanyang.ac.kr](mailto:kima@hanyang.ac.kr)

Received 23 October 2015, revised 11 February 2016

Accepted for publication 17 March 2016

Published 11 April 2016



CrossMark

## Abstract

In this work, combined silver/copper nanoparticles were fabricated by the electrical explosion of a metal wire. In this method, a high electrical current passes through the metal wire with a high voltage. Consequently, the metal wire evaporates and metal nanoparticles are formed. The diameters of the silver and copper nanoparticles were controlled by changing the voltage conditions. The fabricated silver and copper nano-inks were printed on a flexible polyimide (PI) substrate and sintered at room temperature via a flash light process, using a xenon lamp and varying the light energy. The microstructures of the sintered silver and copper films were observed using a scanning electron microscope (SEM) and a transmission electron microscope (TEM). To investigate the crystal phases of the flash-light-sintered silver and copper films, x-ray diffraction (XRD) was performed. The absorption wavelengths of the silver and copper nano-inks were measured using ultraviolet–visible spectroscopy (UV–vis). Furthermore, the resistivity of the sintered silver and copper films was measured using the four-point probe method and an alpha step. As a result, the fabricated Cu/Ag film shows a high electrical conductivity ( $4.06 \mu\Omega\text{cm}$ ), which is comparable to the resistivity of bulk copper ( $1.68 \mu\Omega\text{cm}$ ). In addition, the fabricated Cu/Ag nanoparticle film shows superior oxidation stability compared to the Cu nanoparticle film.

**Keywords:** copper and silver nano-ink, wire explosion, flash light sintering, low porosity, printed electronics

(Some figures may appear in colour only in the online journal)

## 1. Introduction

Metal nano-ink is used in applications such as flexible radio frequency identification (RFID) tags, active-matrix LCDs, e-paper, flexible organic light emitting diodes (OLEDs), and wearable electronics [1–5]. Metal nano-ink consists of metal nanoparticles, an organic binder, a precursor, and a solvent.

The most important components of metal nano-ink are the metal nanoparticles. To synthesize metal nanoparticles, various methods have been used such as polyol processes [6, 7], gas phase condensation [8, 9], thermal plasma [10, 11], and wire explosion [12–14]. In the polyol process and gas phase condensation methods, the particle size and shape can be elaborately controlled [8, 9]. However, the many chemical

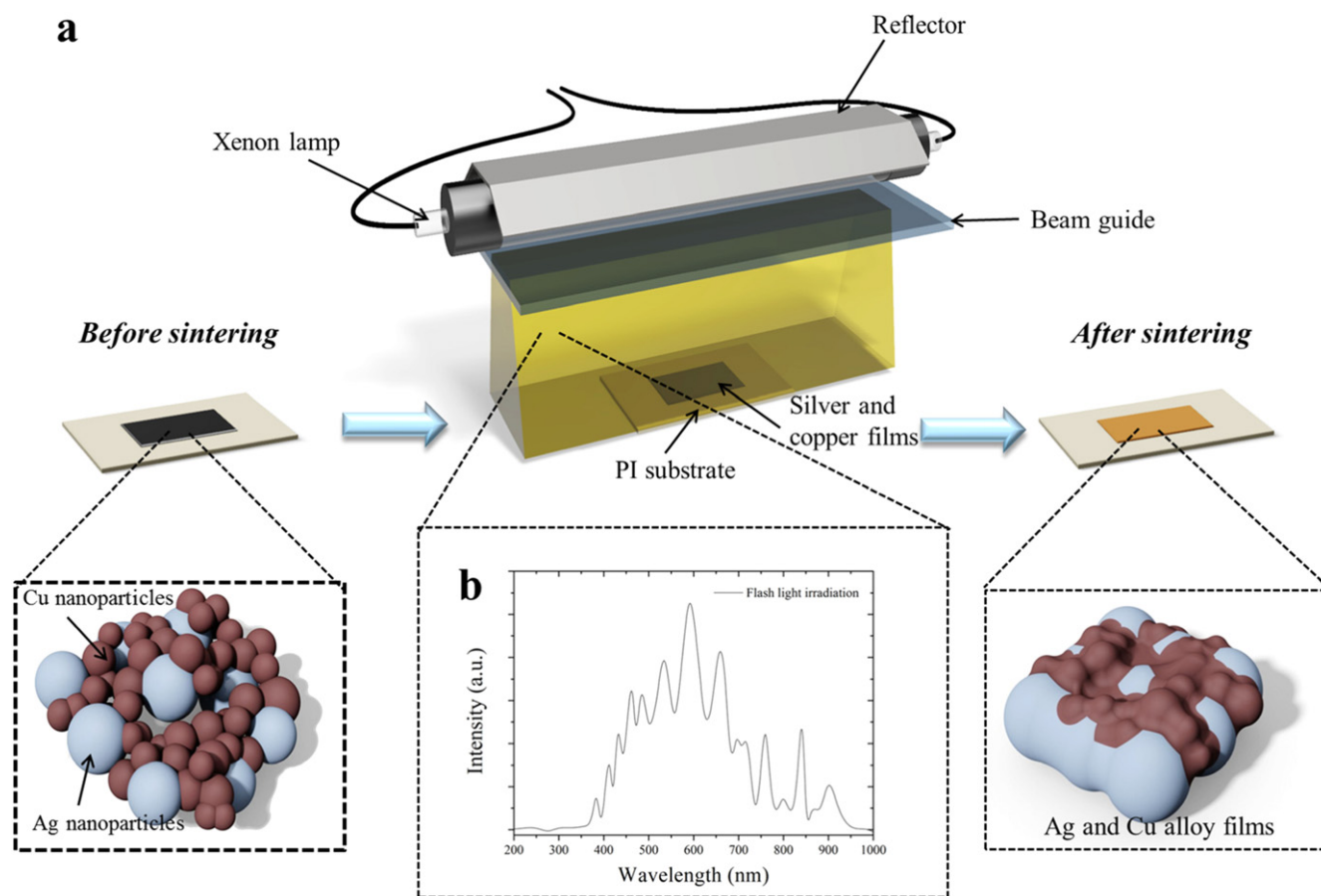


**Figure 1.** (a) The schematics of the flash white light sintering process and (b) the spectrum wavelength of a flash white light from a xenon lamp.

reactions required and low throughput rate are shortcomings regarding mass production. The thermal plasma method also requires a complex process system with a high energy density, namely strong gradients between the medium carrying the deposition precursor and the surroundings [10, 11]. The wire explosion process has many advantages, such as the simplicity of the process, having a rapid production speed and having a high throughput rate, which are appropriate for mass production in industry. Furthermore, in the wire explosion process, it is easy to fabricate different nanoparticles together in the same solution simply by changing the metal wire used in the process. One problem with the wire explosion process is the non-uniform size of the metal nanoparticles generated from the nano and micro particles. However, the non-uniform size distribution of the metal particles may be more suitable than uniform nanoparticles in the sintering process, as the sintering characteristics of bimodal particles with nano and micro metal particles (e.g. copper) showed better sintering characteristics in our previous study [15]. Therefore, in this study, the wire explosion technique has been used for the fabrication of Cu/Ag combined nano-ink.

The low price, high conductivity and high oxidation resistance are also important issues in printed electronics. However, gold, silver and copper are not suitable for satisfying these three demands simultaneously [16]. Note that silver and

gold are too expensive, in spite of their oxidation resistance. Meanwhile, copper nanoparticles are cheap, but vulnerable to oxidation [17]. Therefore, in this study, copper and silver nanoparticles have been developed to satisfy all demands such as low price, high conductivity and oxidation resistance.

To achieve the high conductivity of the metal nano-ink, various sintering techniques, such as thermal [18], laser [19] and microwave processes [20], have been used. These conventional approaches have limitations such as a low throughput, high complexity, and considerable environmental obstacles (e.g. high temperature or vacuum conditions). To solve these problems, we previously developed a flash white light sintering method [21–24]. The flash light sintering method can sinter the nano-ink in a few milliseconds, removing the oxide shells of copper nanoparticles at room temperature and under ambient conditions, without damaging the substrate [24].

In this study, to form and disperse the copper and silver nanoparticles simultaneously, several variables, such as the explosion voltage and solvent, were changed in the wire explosion process. Thus, it was demonstrated that the Cu/Ag combined nanoparticle ink could be obtained by a one-step wire explosion process. Furthermore, to achieve the high electrical conductivity of Cu/Ag combined nano-ink patterns, the flash white light irradiation conditions, such as the

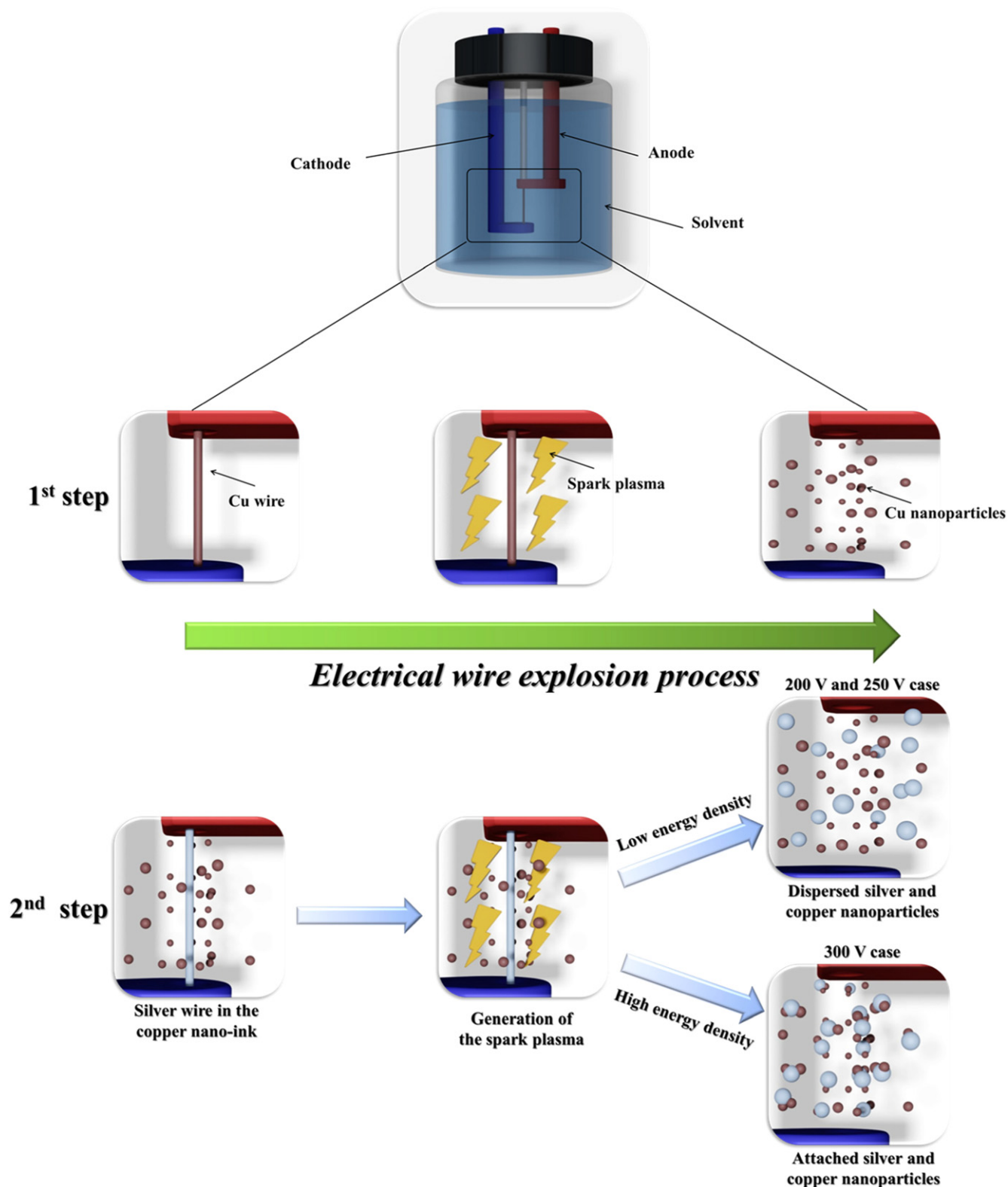


**Figure 2.** The schematics of the fabricated silver and copper ink by the electrical wire explosion process.

irradiation energy and pulse duration, were optimized. The sintered Cu/Ag combined nano-ink patterns were characterized using scanning electron microscopy (SEM), transmission electron microscopy (TEM), UV-visible spectrometry (UV-

vis), and x-ray diffraction (XRD). Also, to evaluate the high electrical conductivity and oxidation stability, the sheet resistance of the sintered Cu/Ag combined nano-ink patterns was measured using a four-probe method.

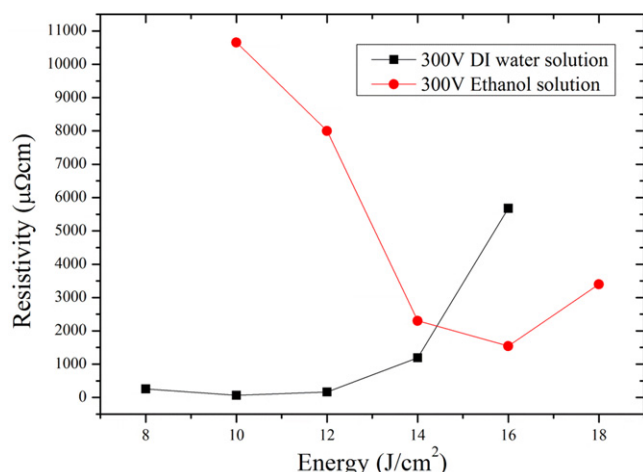


**Figure 3.** The resistivity of the sintered copper films for the base solvent of the electrical wire explosion process.

## 2. Experiment details

### 2.1. The fabrication of Cu/Ag combined nano-ink using the wire explosion process

First, to fabricate the silver and copper nanoparticles, copper wire (diameter: 0.12 mm, length: 32 mm) was exploded in 500 ml of solvent (distilled water or ethanol) under various voltages (200, 250, and 300 V) in the electrical wire explosion process. Then, a silver wire (diameter: 0.2 mm, length: 32 mm) was immersed in the copper particle solution, and exploded in the same manner. To separate the micro-sized particles ( $>1 \mu\text{m}$ ), the fabricated Cu/Ag solution was filtered using a mesh filter with a mesh hole size of less than  $1 \mu\text{m}$ . A centrifuge was used for 1 h to collect the silver and copper particles in the solution. For the Cu/Ag combined nano-ink formulation, the collected silver and copper nanoparticles were dispersed in a diethylene glycol (DEG, 99%; Samchun Chemical) (0.7 g) solvent with dissolved poly (*N*-vinylpyrrolidone) (PVP, MW 55 000; Sigma Aldrich) (0.07 g) by an ultra-sonicator for 1 h.

### 2.2. Preparation of combined Cu/Ag nano-ink films

A polyimide (PI) film with a thickness of  $225 \mu\text{m}$  was used as the substrate film. To remove contamination, the PI substrate was cleaned in ethanol and distilled water using an ultra-sonicator for 10 min. The Cu/Ag combined nano-inks were printed on the PI substrate using the doctor blade method. The printed patterns were  $2 \text{ cm}$  (length)  $\times$   $1 \text{ cm}$  (width). Then, the printed patterns were dried on a hot plate ( $80^\circ\text{C}$ ) for 1 h.

### 2.3. Flash light sintering of silver and copper films

The printed Cu/Ag combined nano-ink patterns were sintered by an in-house flash light sintering system at room temperature under ambient conditions. The flash light sintering system consisted of a xenon lamp (Perkin-Elmer Co.), a power supply, capacitors, a pulse controller, and a reflector

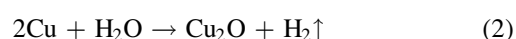
(figure 1). The emitted white light from the xenon lamp has a wide range of wavelengths from 380 to 950 nm (figure 1(b)) [22, 25]. The flash light energy was controlled from 8 to  $14 \text{ J cm}^{-2}$ , while the pulse duration and pulse number were fixed at 10 ms and 1, respectively.

### 2.4. Characterization

The microstructures of the Cu/Ag combined nano-ink patterns were observed using a scanning electron microscope with an operating voltage of 15 kV (SEM, S4800 HITACHI). To investigate the oxidation or reduction of the sintered patterns, crystal phase analysis was performed by x-ray diffraction (XRD, D/MAX RINT 2000, Cu  $K\alpha$  radiation) with an operating voltage of 40 kV, a current of 60 mA, and Bragg-Brentano geometry. The light absorption of the Cu/Ag combined nano-ink was analyzed using a UV-visible spectrometer (UV-vis, S-4100, Scinco). The shapes and sizes of the silver and copper nanoparticles were observed using a transmission electron microscope (TEM, JEM 2100F, JEOL). The thicknesses of the patterns for resistivity calculations were measured using an Alpha-Step surface profiler (KLA Tencor AS500, Tencor Instruments) (thickness:  $4 \mu\text{m}$ ).

## 3. Results and discussion

The electrical wire explosion process was conducted in DI water or ethanol under various conditions (voltage: 300 V, pulse number: 1000) (figure 2). First, only copper nanoparticles were fabricated. For the sintering of the fabricated copper nano-ink, the flash light from a xenon lamp was irradiated on the film. In the case of the ethanol solvent, the resistivity of the sintered copper films decreased as the flash light energy was increased from  $10 \text{ J cm}^{-2}$  to  $16 \text{ J cm}^{-2}$  (figure 3). However, for flash light energies higher than  $16 \text{ J cm}^{-2}$ , the resistivity of the sintered copper pattern increased, as the copper films were burned by excessive light energy [26] (figure 4). Meanwhile, in the case of the DI water, the resistivity of the copper films sintered at  $10 \text{ J cm}^{-2}$  was lower than the resistivity obtained in the other flash light energy cases. Also, at flash light irradiation of  $10 \text{ J cm}^{-2}$ , the resistivity of the sintered copper films of the DI water case ( $64.56 \mu\Omega\text{cm}$ ) was much lower than that of the sintered copper films of the ethanol case ( $1.54 \text{ m}\Omega\text{cm}$ ). This is because when the copper nanoparticles generated in the ethanol solution were sintered, a lot of holes or craters were generated on the surface of the copper films (figure 4). Figure 5 shows the XRD results of the copper nano-ink films fabricated in DI water and ethanol solvents. A copper carbide peak was observed in the case of the ethanol solution. Therefore, it can be concluded that copper carbides and copper oxide were generated when the copper wire was exploded in the ethanol solvent—as shown in the following formulas (1) and (2)—due to the carbon ions of ethanol [25, 27]:





Base solvent	Flash white light irradiation energy					
	8 J/cm <sup>2</sup>	10 J/cm <sup>2</sup>	12 J/cm <sup>2</sup>	14 J/cm <sup>2</sup>	16 J/cm <sup>2</sup>	18 J/cm <sup>2</sup>
Ethanol						
DI water						

**Figure 4.** A photograph of the sintered copper films for the base solvent of the electrical wire explosion process and flash white light energy conditions.

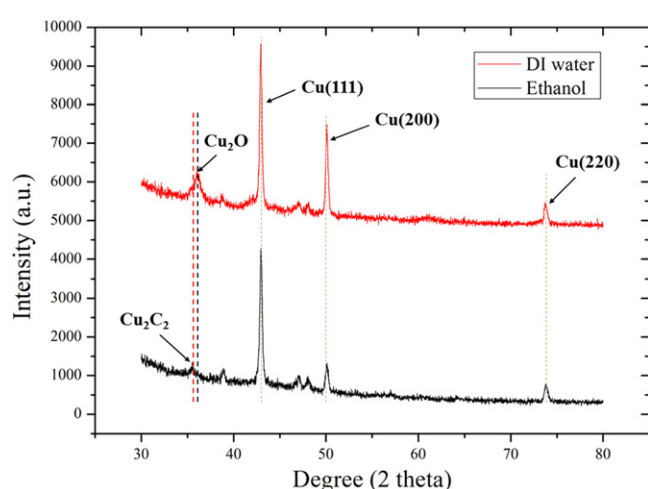


**Figure 5.** The XRD patterns of copper nanoparticles fabricated for the base solvent of the electrical wire explosion process.

The fabricated copper carbide has dangerous properties such as its ability to explode easily given a small external energy [28]. The highly explosive copper carbide is not appropriate in printed electronics because the explosive decomposition of copper carbide with the unstable bonds of copper and carbon ions can be initiated by thermal heating over 120 °C, an impact, or electric spark [29]. In the flash light sintering process, the copper carbide nanoparticles would be exploded by the flash light irradiation and this would be followed by delamination and crater generation on the surface of the copper films. For this reason, it was concluded that DI water was suitable for the fabrication of copper nanoparticles in the wire explosion process.

To control the size of the copper nanoparticles, the explosion voltage of the electrical wire explosion process was changed from 200 V to 300 V. As shown in the SEM images in figures 6(b)–(d), the size of the copper nanoparticles decreased from 45 nm to 17 nm as the applied voltage to the copper wire was increased. The fabricated copper nano-ink was sintered by various amounts of flash light irradiation energy. After irradiation with a flash light energy of 10 J cm<sup>-2</sup>, the sintered copper films showed the lowest resistivity for all cases. Meanwhile, as the size of the copper

nanoparticles decreased, the resistivity of the copper films sintered at the flash light energy of 10 J cm<sup>-2</sup> also decreased (figure 6(a)). This could be because as the size of the nanoparticles decreases, they become more densely packed, and porosity thus also decreases (figures 6(e)–(g)). Therefore, to fabricate the copper nano-ink, the applied voltage chosen for the exploding copper wire was 300 V.

To control the size of the silver nanoparticles, the silver wire was exploded under various applied voltages ranging from 200 V to 300 V. The SEM images in figures 7(b)–(d) show the sizes of the silver nanoparticles in the fabricated silver nano-ink. The size of the silver nanoparticles decreased from 74.1 nm to 48.3 nm as the applied voltage to the silver wire was increased. The silver nanoparticles are larger than the copper nanoparticles. The size of the fabricated metal nanoparticles in the wire explosion process was determined by various parameters such as the diameter and length of the metal wire and the energy applied to it. Because the applied energy in the metal wire increased, as the voltage of the wire explosion process was increased, the size of the fabricated metal nanoparticles decreased. The minimum energy needed to cause the explosion of the metal wire can be determined using formulas (3) and (4) [30].

$$W = V_{\text{metal}} \times w_s, \quad (3)$$

$$V_{\text{metal}} = \pi \times d^2 \times l/4, \quad (4)$$

where  $W$  is the minimum energy needed to explode the metal wire,  $V_{\text{metal}}$  is the volume of the metal wire,  $w_s$  is the evaporation energy of the metal,  $d$  is the diameter of the metal wire, and  $l$  is the length. In this work, the diameter of the silver wire (0.2 mm) was larger than that of the copper wire (0.12 mm) and the evaporation energy of the copper (47.5 J mm<sup>-3</sup>) was higher than that of the silver (27.8 J mm<sup>-3</sup>) (table 1). The calculated minimum energy needed to explode the silver wire (27.93 J) was higher than for the copper wire (17.18 J). Therefore, for the same wire explosion energy, larger silver nanoparticles compared to copper nanoparticles could be obtained.

The fabricated silver nano-ink was sintered under various amounts of flash light irradiation energy. In the case of a flash light energy of 6 J cm<sup>-2</sup>, the sintered silver films showed the

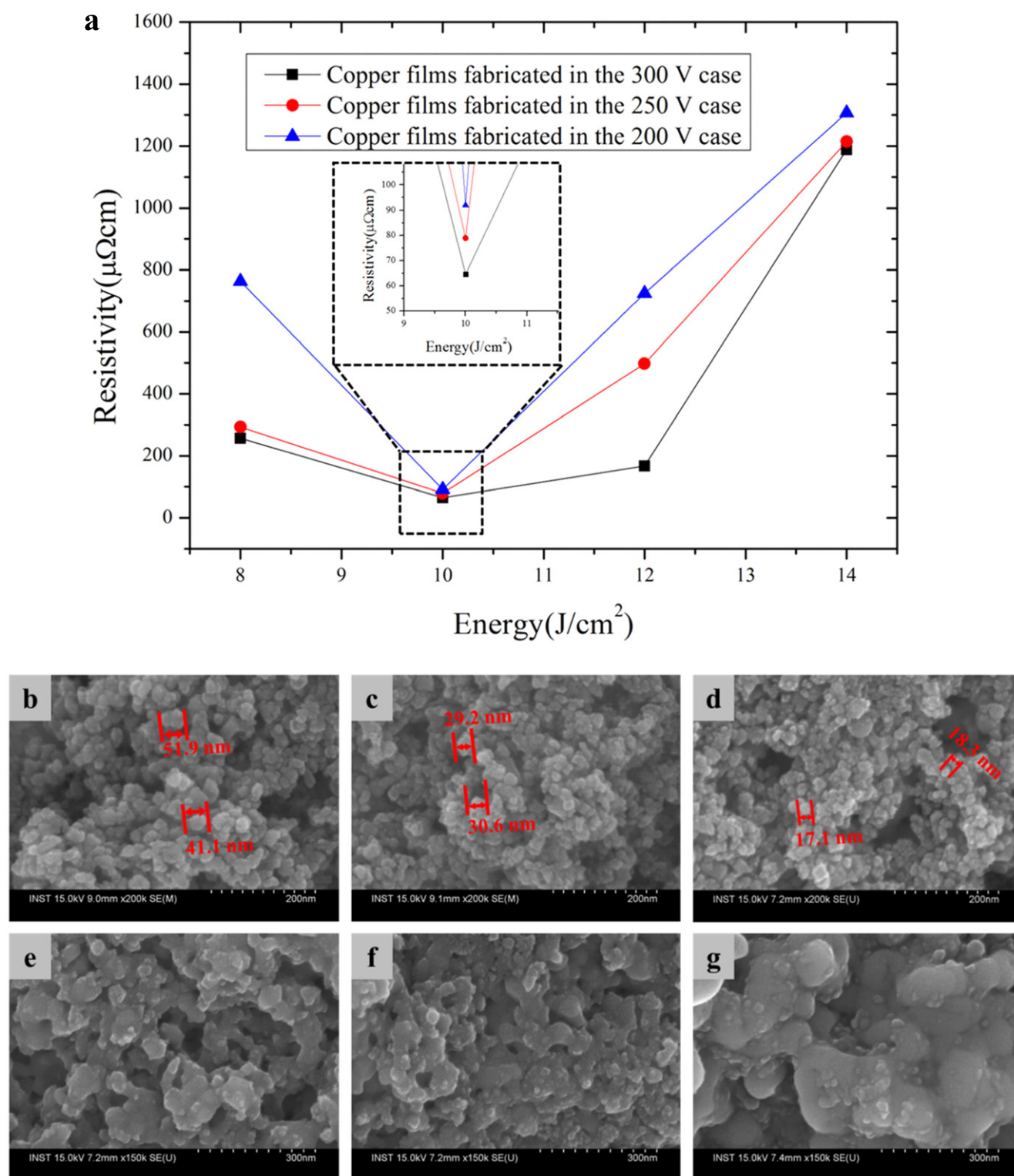


**Figure 6.** (a) The resistivity of pure copper films for flash white light irradiation energy and the SEM image of the copper films fabricated by the electrical wire explosion of (a) and (d) 200 V; (b) and (e) 250 V; (c) and (f) 300 V ((b)–(d): unsintered copper films and (e)–(g): sintered copper films with an energy of  $10 \text{ J cm}^{-2}$  for 10 ms).

lowest resistivity. Also, as the size of the silver nanoparticles decreased, the resistivity of the sintered silver films at the flash light energy of  $6 \text{ J cm}^{-2}$  decreased (figure 7(a)). In both the copper and silver films, it was found that the resistivity of the sintered film decreased as the size of the metal

nanoparticles decreased. It was also found that the resistivity of the sintered silver films was lower than that of the sintered copper films. However, silver is not appropriate for the mass production of printed electronics due to its high price. Therefore, silver and copper nanoparticles were used

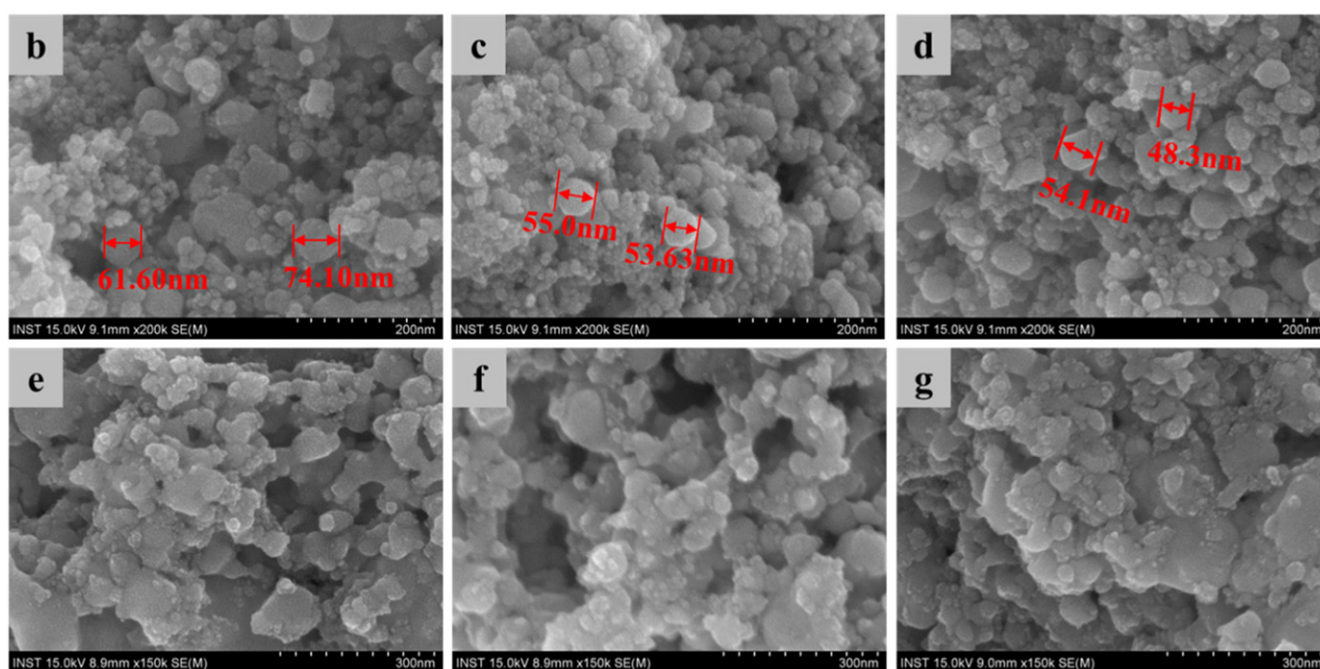
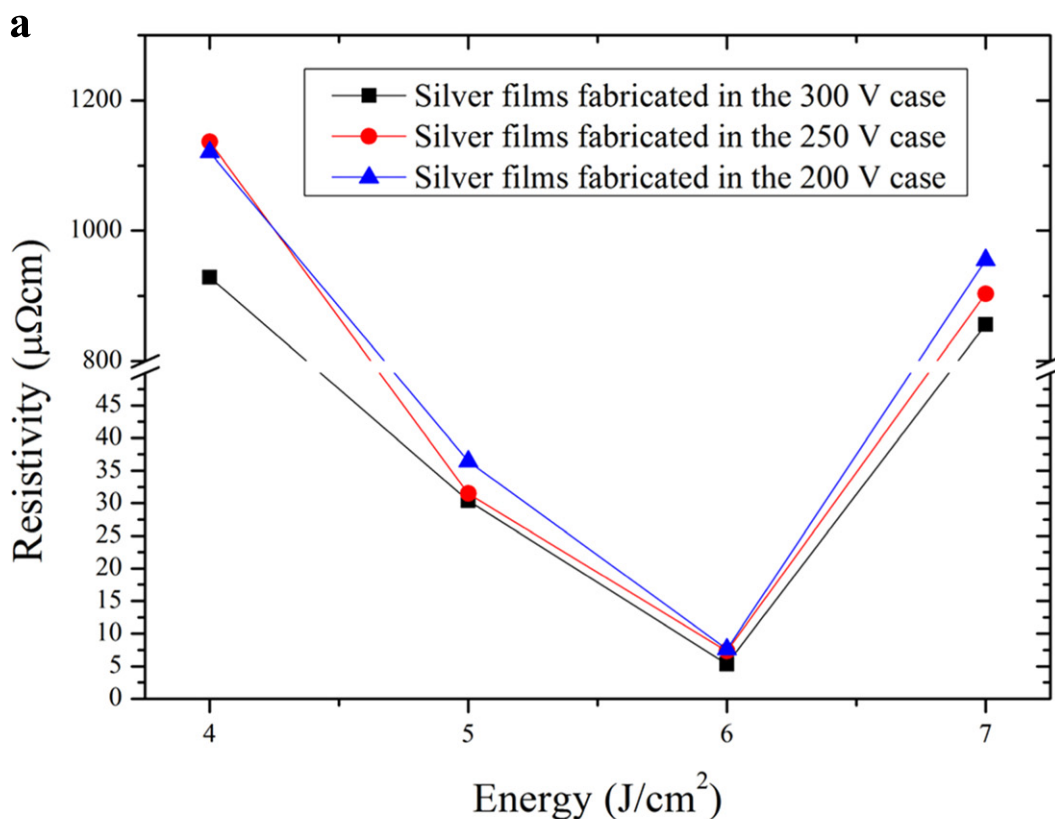


**Figure 7.** (a) The resistivity of pure silver films for flash white light irradiation energy and the SEM image of the silver films fabricated by the electrical wire explosion of (b) and (e) 200 V; (c) and (f) 250 V; (d) and (g) 300 V ((b)–(d): unsintered silver films and (e)–(g): sintered silver films with an energy of  $10 \text{ J cm}^{-2}$  for 10 ms).

simultaneously. To fabricate metal-ink with mixed copper and silver nanoparticles, the silver wire was immersed in a copper solution fabricated in DI water at an applied voltage of 300 V and exploded under various voltages (e.g., 200 V, 250 V, and 300 V) with silver (50 wt%) and copper (50 wt%). Figure 8(a) shows the resistivity of the sintered Cu/Ag combined nano-

ink films with different nanoparticle sizes. As shown in figure 8(a), the sintered Cu/Ag combined nano-ink films show the lowest resistivity when a flash light energy of  $10 \text{ J cm}^{-2}$  was applied. Meanwhile, as the applied voltage to the silver wire was increased, the resistivity of the sintered Cu/Ag combined nano-ink films decreased. This is because



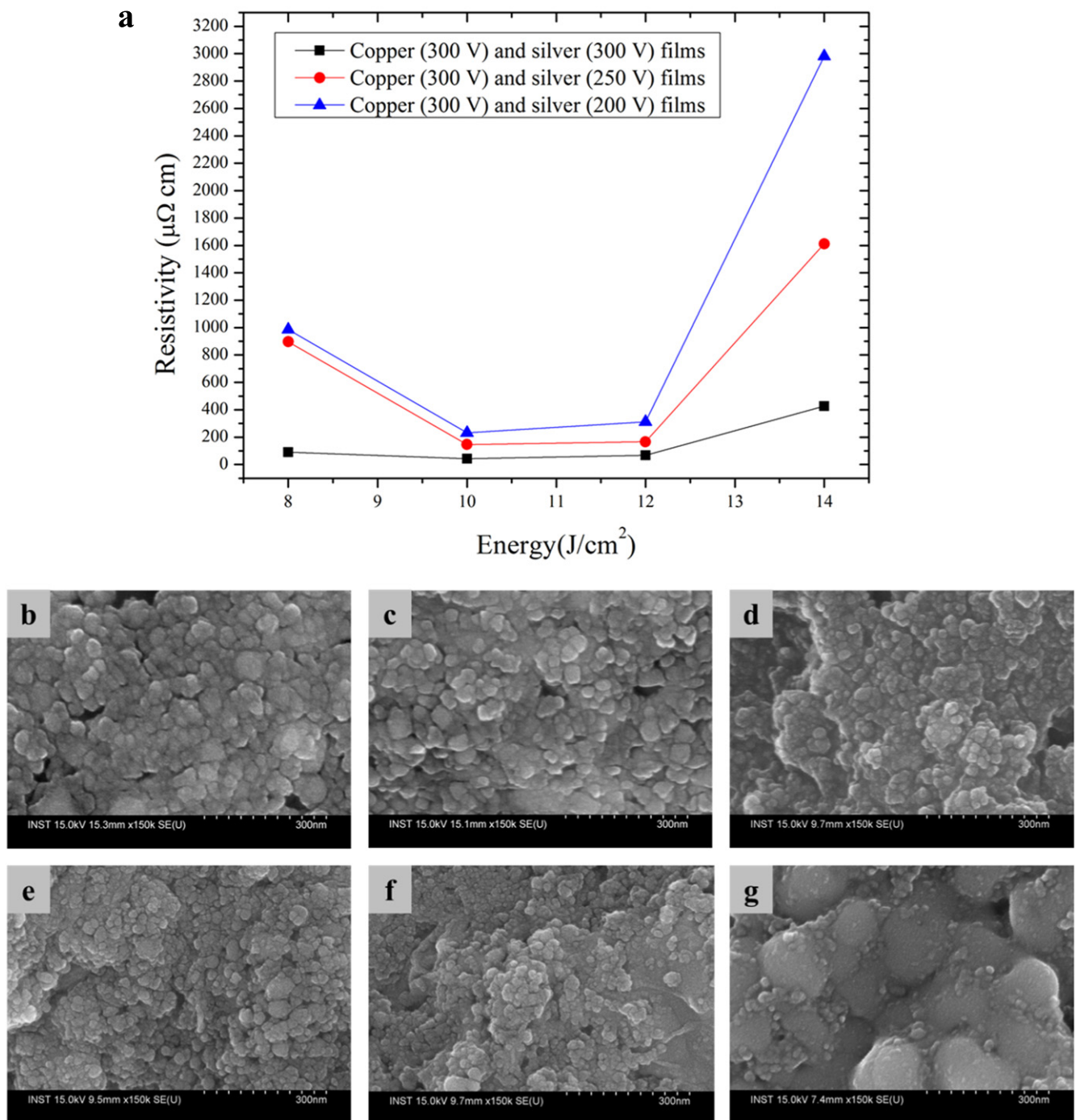


**Figure 8.** (a) The resistivity of Cu/Ag combined nano-ink films for flash white light energy and the SEM image of the silver and copper films fabricated by the electrical wire explosion of (b) and (e) 300 V and 200 V; (c) and (f) 300 V and 250 V; (d) and (g) 300 V and 300 V ((a)–(c): unsintered silver and copper films and (d)–(f): sintered silver and copper films with an energy of  $10 \text{ J cm}^{-2}$  for 10 ms).

**Table 1.** The various parameters for exploding metal wire via the electrical wire explosion process.

	Diameter of wire ( $d$ , mm)	Length of wire ( $l$ , mm)	Evaporation energy of metal ( $w_s$ , $\text{J mm}^{-3}$ )	Minimum energy to evaporate metal wire ( $W$ , J)
Silver	0.2	32	27.8	27.93
Copper	0.12	32	47.5	17.18

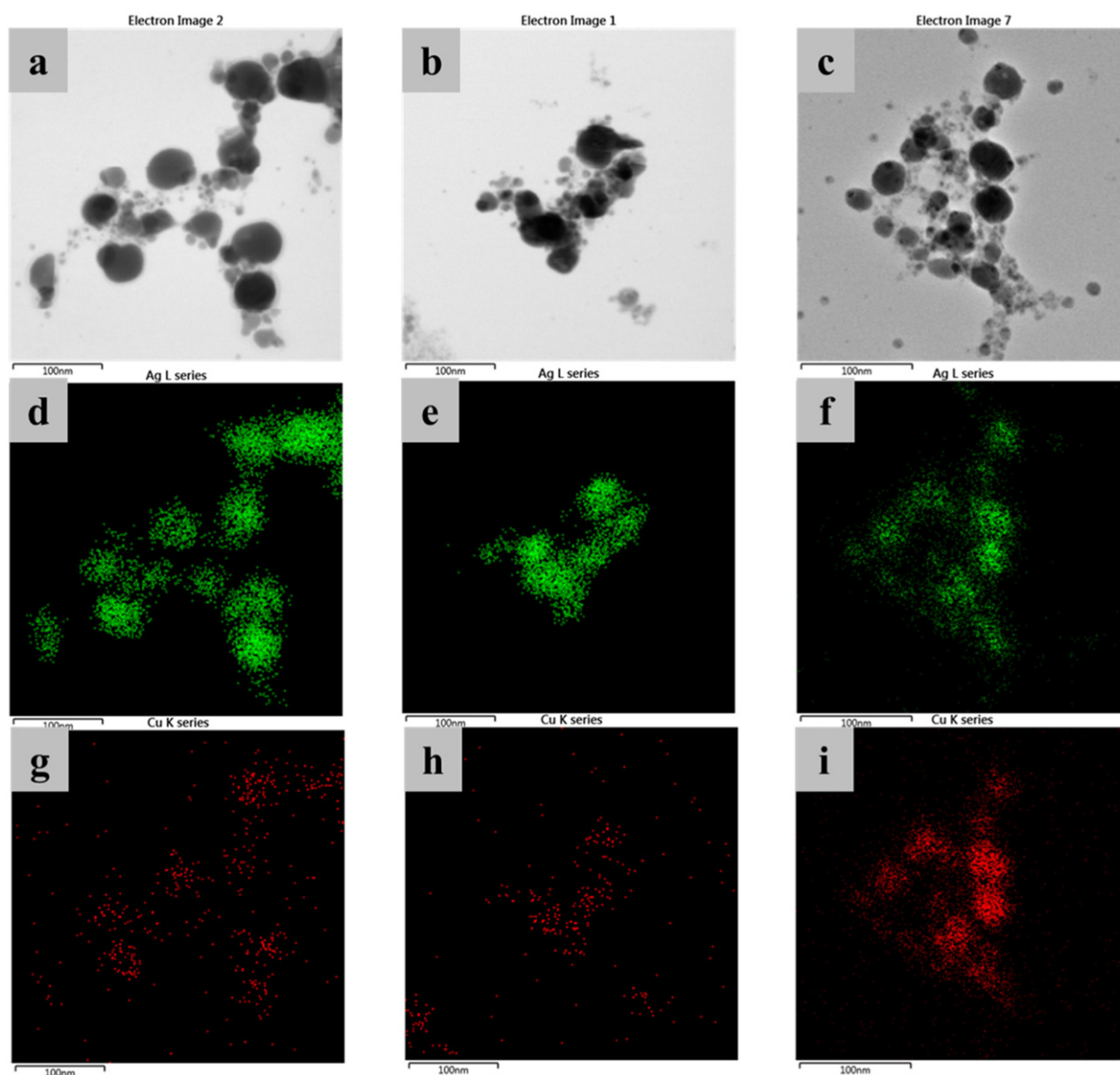


**Figure 9.** The TEM image of Cu/Ag combined nano-ink fabricated in the case of (a) 200 V, (b) 250 V and (c) 300 V, the mapping image of silver among the copper and silver ink fabricated in the case of (d) 200 V, (e) 250 V and (f) 300 V, and the mapping image of copper among the copper and silver ink fabricated in the case of (g) 200 V, (h) 250 V and (i) 300 V.

the size of the fabricated silver nanoparticles became smaller and the pores of the sintered Cu/Ag nano-inks films were reduced as the applied voltage was increased (figures 8(e)–(g)).

To determine the size and the distribution of the silver and copper nanoparticles in the Cu/Ag combined nano-ink, TEM analysis was conducted. For wire explosion conditions of 200 V and 250 V, the mapping points of small copper (red color) nanoparticles were spread from those of the large silver nanoparticles (green color) (figures 9(g) and (h)), demonstrating that they were separately dispersed. Meanwhile, for the wire explosion condition of 300 V, the mapping images of tiny copper nanoparticles were found on the surfaces of the large silver nanoparticles (figures 9(c), (f), and (i)). This means that the silver and copper nanoparticles were attached together in the case of the voltage of 300 V. This phenomenon may occur during the spark plasma in the wire explosion

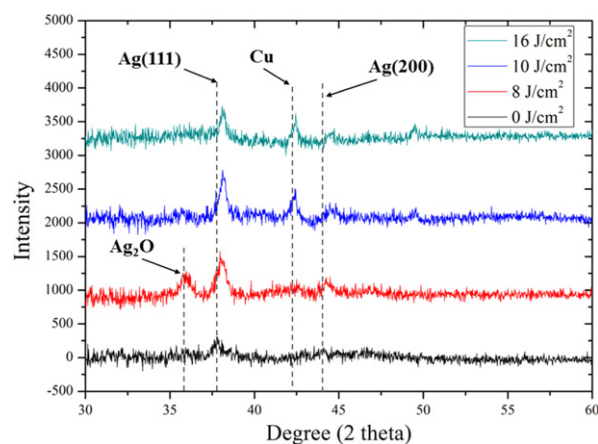


**Figure 10.** The XRD patterns of silver and copper films for flash white light energy (wire explosion condition: silver (300 V) and copper (300 V)).

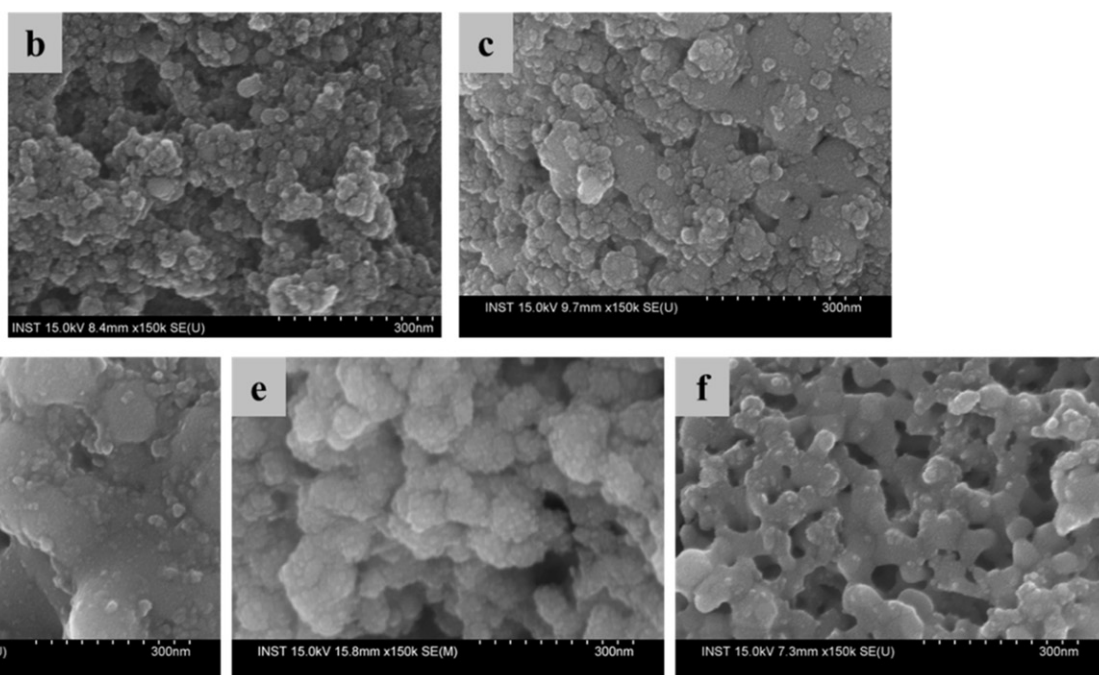
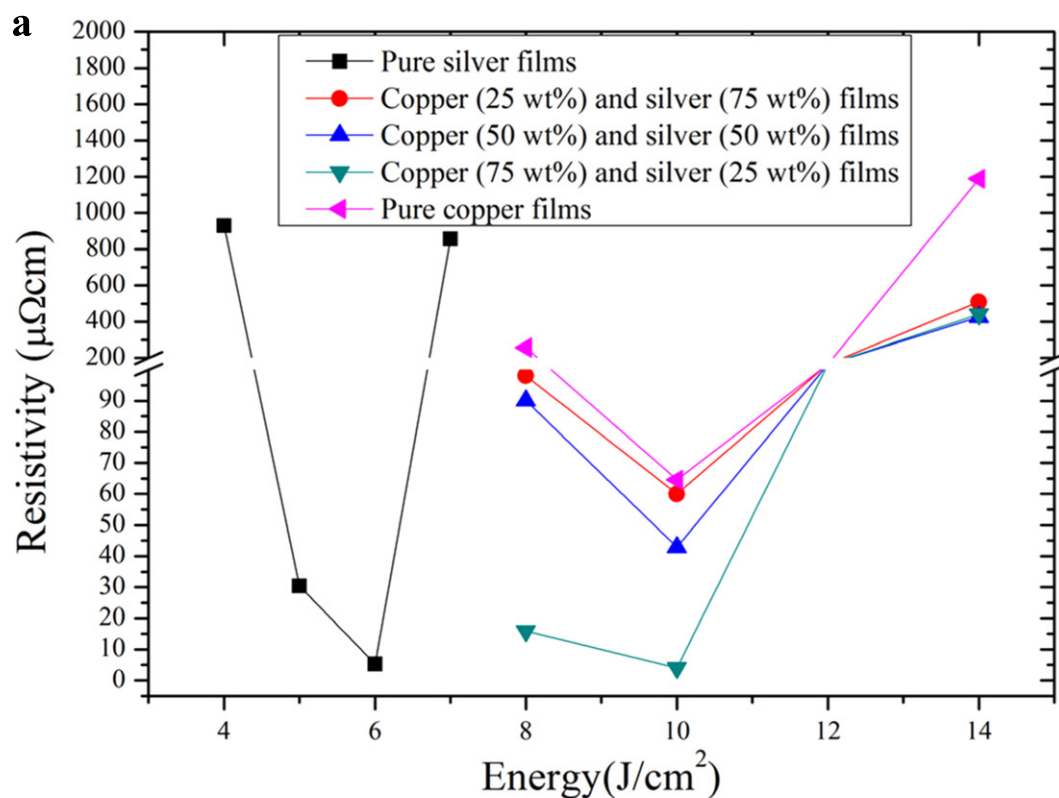


**Figure 11.** The resistivity of the sintered Cu/Ag combined nano-ink films for the weight fraction and the SEM image of the silver (25 wt%) and copper (75 wt%) films for (b) unsintered, (c)  $8 \text{ J cm}^{-2}$ , (d)  $10 \text{ J cm}^{-2}$ , (e)  $12 \text{ J cm}^{-2}$ , and (f)  $14 \text{ J cm}^{-2}$ .

process, and it is illustrated by the schematics shown in figure 2. When the silver wire exploded, silver nanoparticles formed as the evaporated wire was quickly condensed in DI water, and simultaneously attached to the copper nanoparticles with a high energy density [31–33]. However, when low voltages were applied to the silver wire, the silver and

copper nanoparticles did not attach due to the low spark plasma energy. Therefore, in this study, an applied voltage of 300 V for both the copper and silver wires was chosen in the wire explosion process in order to achieve smaller silver nanoparticles uniformly attached and surrounded by tiny copper nanoparticles.



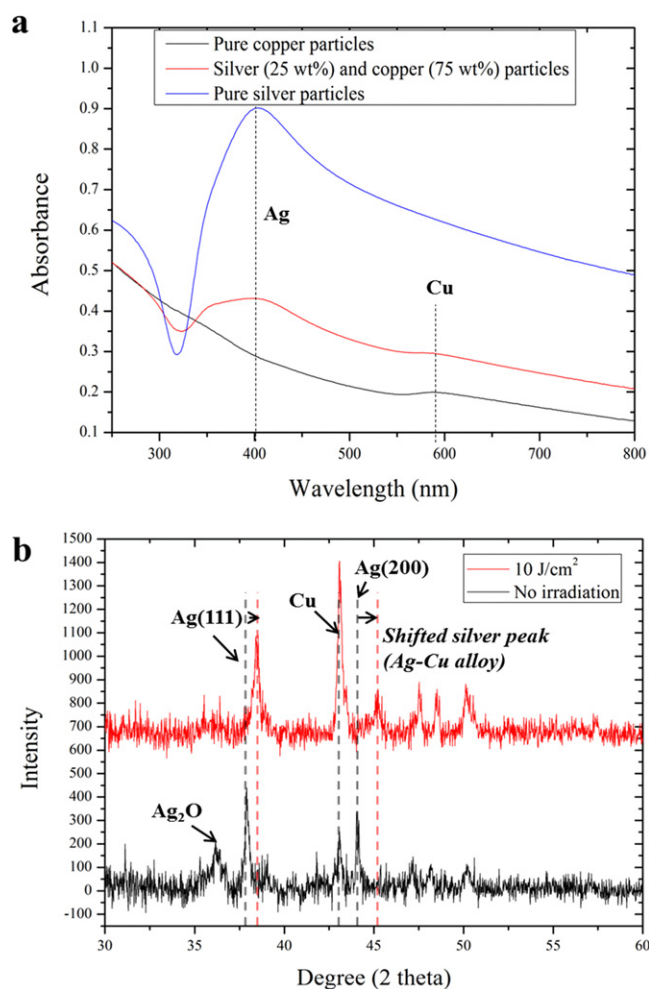


**Figure 12.** (a) The UV-vis data of silver, copper and silver (25 wt%) and copper (75 wt%) particles and (b) the XRD patterns of the Cu/Ag combined nano-ink films before and after flash white light sintering.

Figure 10 shows the XRD data of the Cu/Ag combined nano-ink fabricated at an applied voltage of 300 V before and after sintering. In the XRD data before sintering the Cu/Ag combined nano-ink, copper, copper oxide, silver, and silver oxide peaks were observed. Before sintering, the copper peak had a lower intensity than the silver peak as the silver nanoparticles were larger than the copper nanoparticles. However, with the increasing irradiation energy of the flash light, the copper peak increased due to the increased size of the sintered copper nanoparticles. It is noteworthy that the silver and copper oxide peaks totally disappeared at  $10 \text{ J cm}^{-2}$  (figure 10) due to the reduction phenomenon of copper and silver oxides by the intermediate alcohol decomposed from PVP during the flash white light irradiation, as reported in previous work (chemical formulas (5) and (6)) [25, 34]:

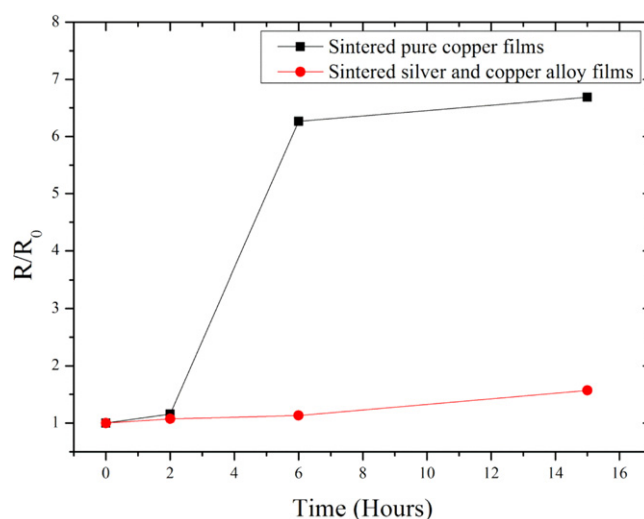
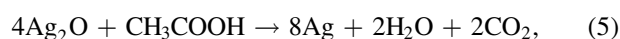


**Figure 13.** The resistivity of sintered pure copper films and Cu/Ag combined nano-ink films for an increasing time at  $100^\circ\text{C}$ .

As a result, the silver and copper nanoparticles reduced from silver and copper oxide were sintered and the pores were filled among them (figure 8(g)).

To optimize the weight fractions of silver and copper nanoparticles in the Cu/Ag combined nano-ink, the explosion numbers of the wires were varied from 750 to 250 (total explosion number: 1000). The fabricated silver and copper inks were sintered by the flash light. As shown in figure 11(a), the Cu/Ag combined nano-ink sintered at the irradiated flash light energy of  $10 \text{ J cm}^{-2}$  showed the lowest resistivity in all cases, regardless of the weight fractions of silver and copper. It is noteworthy that the sintered Cu/Ag combined nano-ink (Cu (75 wt%):Ag (25 wt%)) films showed the lowest resistivity ( $4.06 \mu\Omega\text{cm}$ ), this being even lower than that of the sintered pure silver films ( $5.3 \mu\Omega\text{cm}$ ). Furthermore, in the SEM image of silver (25 wt%) and copper (75 wt%) films, as the flash light energy was increased up to  $10 \text{ J cm}^{-2}$ , the pores of the Cu/Ag combined nano-ink films were removed and the sizes of the Cu/Ag combined nano-particles were increased (figures 11(b)–(d)). Meanwhile, when the irradiated flash white light energy was higher than  $10 \text{ J cm}^{-2}$ , many pores on the surface of the silver and copper films were generated due to the excessive energy (figures 11(e) and (f)). The silver and copper nanoparticles were sintered due to the photothermal effects generated by the irradiated flash white light. Such photothermal effects may be ascribed to surface plasmon resonance, whereby absorbed photons are converted into phonons in the silver and copper nanoparticles after light exposure [25, 35]. To analyze the absorbance wavelength of the silver and copper nanoparticles, a spectrophotometer was employed. In the UV-vis results shown in figure 12(a), two peaks of the plasmonic wavelength of the Cu/Ag combined nano-ink were observed at 400 nm and 580 nm [36, 37], while only one peak was observed in the pure silver and copper nano-inks. The flash light from the xenon lamp used in this study has a wavelength range of 350 nm to 850 nm, which



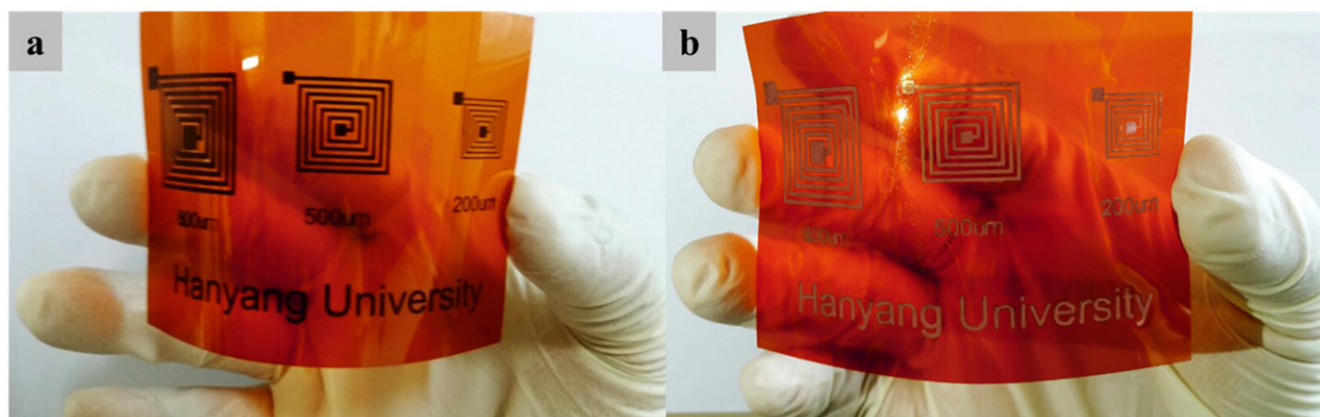


**Figure 14.** The printed silver and copper films on the PI substrate using the screen printing method (a) before flash white light irradiation, (b) after flash white light irradiation.

covers the plasmonic wavelengths of Cu/Ag (figure 1(b)). Therefore, the double plasmonic peaks in the Cu/Ag nano-ink would accelerate the photothermal effect during the irradiation of the flash light, which could enhance the sintering efficiency in the flash light sintering process (figure 11).

As shown in the XRD data in figure 12(b), the silver and copper oxide peaks decreased because they were reduced by the irradiated flash light. Also, after the flash light irradiation, the silver peaks ( $37.9^\circ$  and  $44.04^\circ$ ) of the (111) and (222) directions shifted to the right-hand side ( $38.42^\circ$  and  $45.22^\circ$ ) [38], respectively. This is because when the flash light was irradiated on the Cu/Ag nano-ink films, surface plasmon resonance was generated in the silver and copper nanoparticles followed by the melting and forming of a Cu/Ag alloy.

To evaluate the oxidation resistance of the sintered Cu/Ag nano-ink films, the sintered Cu/Ag combined nano-ink films were subjected to a high temperature in a furnace ( $100^\circ\text{C}$ ) and their resistivity was measured every 2 h and compared to that of a pure Cu film. Figure 13 shows the resistivity results after sintering the silver and copper films. After 2 h, the resistivity of the pure copper films abruptly increased due to oxidation, while the Cu/Ag combined nano-ink film retained its original resistance. It is well known that the resistance against oxidation of the Cu/Ag alloy was much higher than that of pure copper [39]. Figure 14 shows the Cu/Ag nano-ink films before and after sintering. It is expected that the Cu/Ag combined nano-ink will be widely used in printed electronics for reliable oxidation proof applications.

#### 4. Conclusion

In this study, Cu/Ag combined nano-inks were fabricated using an electrical wire explosion process and sintered via flash white light irradiation to achieve a highly conductive electrode pattern. The sizes of the silver and copper nanoparticles fabricated by the process were optimized for flash white light sintering. Furthermore, it was possible to use the optimized flash light sintering process to sinter the silver and copper films. The sintered silver (25 wt%) and copper

(75 wt%) films demonstrated high resistance against oxidation with a low resistivity ( $4.06\ \mu\Omega\text{cm}$ ).

#### Acknowledgments

This work was supported by the Nano-Convergence Foundation ([www.nanotech2020.org](http://www.nanotech2020.org)) funded by the Ministry of Science, ICT and Future Planning (MSIP, Korea) and the Ministry of Trade, Industry and Energy (MOTIE, Korea) (Project Number: R201502510). This research was also supported by the Basic Science Research Program through the National Research Foundation of Korea (NRF) funded by the Ministry of Education (2012R1A6A1029029). This work was supported by the Technology Innovation Program (and the Industrial Strategic Technology Development Program, 10048913, for the development of cheap nano-ink sintered in air for smart devices) funded by the Ministry of Trade, Industry and Energy (MI, Korea).

#### References

- [1] Zhang Z, Zhang X, Xin Z, Deng M, Wen Y and Song Y 2011 Synthesis of monodisperse silver nanoparticles for ink-jet printed flexible electronics *Nanotechnology* **22** 425601
- [2] Chen P, Fu Y, Aminirad R, Wang C, Zhang J, Wang K, Galatsis K and Zhou C 2011 Fully printed separated carbon nanotube thin film transistor circuits and its application in organic light emitting diode control *Nano Lett.* **11** 5301–8
- [3] Subramanian V, Chang P C, Lee J B, Moles S E and Volkman S K 2005 Printed organic transistors for ultra-low-cost RFID applications *IEEE Trans. Compon. Packag. Technol.* **28** 742–7
- [4] Zheng Y, He Z, Gao Y and Liu J 2013 Direct desktop printed-circuits-on-paper flexible electronics *Sci. Rep.* **3** 01786
- [5] Lee H M, Choi S Y, Jung A and Ko S H 2013 Highly conductive aluminum textile and paper for flexible and wearable electronics *Angew. Chem.* **125** 7872–7
- [6] Park B K, Jeong S, Kim D, Moon J, Lim S and Kim J S 2007 Synthesis and size control of monodisperse copper nanoparticles by polyol method *J. Colloid Interface Sci.* **311** 417–24

- [7] Zhao Y, Zhu J J, Hong J M, Bian N and Chen H Y 2004 Microwave-induced polyol-process synthesis of copper and copper oxide nanocrystals with controllable morphology *Eur. J. Inorg. Chem.* **2004** 4072–80
- [8] Yamada Y and Castleman A 1993 Gas-phase copper carbide clusters *Chem. Phys. Lett.* **204** 133–8
- [9] Swihart M T 2003 Vapor-phase synthesis of nanoparticles *Cur. Opin. Colloid Interface Sci.* **8** 127–33
- [10] Heberlein J, Postel O, Girshick S, McMurtry P, Gerberich W, Iordanoglou D, Di Fonzo F, Neumann D, Gidwani A and Fan M 2001 Thermal plasma deposition of nanophase hard coatings *Surf. Coat. Technol.* **142** 265–71
- [11] Yabuki A and Arriffin N 2010 Electrical conductivity of copper nanoparticle thin films annealed at low temperature *Thin Solid Films* **518** 7033–7
- [12] Dash P 2010 Generation of nano-copper particles through wire explosion method and its characterization *Res. J. Nanosci. Nanotechnol.* **1** 25–33
- [13] Park S, Her J, Cho D, Haque M M, Park J H and Lee C S 2012 Preparation of conductive nanoink using pulsed-wire-evaporated copper nanoparticles for inkjet printing *Mater. Trans.* **53** 1502–6
- [14] Murai K, Tokoi Y, Suematsu H, Jiang W, Yatsui K and Niihara K 2008 Particle size controllability of ambient gas species for copper nanoparticles prepared by pulsed wire discharge *Japan. J. Appl. Phys.* **47** 3726
- [15] Joo S-J, Hwang H-J and Kim H-S 2014 Highly conductive copper nano/microparticles ink via flash light sintering for printed electronics *Nanotechnology* **25** 265601
- [16] Grouchko M, Kamysnyy A and Magdassi S 2009 Formation of air-stable copper–silver core–shell nanoparticles for inkjet printing *J. Mater. Chem.* **19** 3057–62
- [17] Luechinger N A, Athanassiou E K and Stark W J 2008 Graphene-stabilized copper nanoparticles as an air-stable substitute for silver and gold in low-cost ink-jet printable electronics *Nanotechnology* **19** 445201
- [18] Pan H, Ko S H and Grigoropoulos C P 2008 Thermal sintering of solution-deposited nanoparticle silver ink films characterized by spectroscopic ellipsometry *Appl. Phys. Lett.* **93** 234104
- [19] Beaman J J, McGrath J C and Prioleau F R 1994 Thermal control of selective laser sintering via control of the laser scan *USA Patent Specification* 5352405
- [20] Jiao Z, Shikazono N and Kasagi N 2010 Comparison of ultra-fast microwave sintering and conventional thermal sintering in the manufacturing of anode support solid oxide fuel cell *J. Power Sources* **195** 8019–27
- [21] Park S-H, Jang S, Lee D-J, Oh J and Kim H-S 2013 Two-step flash light sintering process for crack-free inkjet-printed Ag films *J. Micromech. Microeng.* **23** 015013
- [22] Chung W-H, Hwang H-J, Lee S-H and Kim H-S 2013 *In situ* monitoring of a flash light sintering process using silver nano-ink for producing flexible electronics *Nanotechnology* **24** 035202
- [23] Hwang H-J, Chung W-H and Kim H-S 2012 *In situ* monitoring of flash-light sintering of copper nanoparticle ink for printed electronics *Nanotechnology* **23** 485205
- [24] Kim H-S, Dhage S R, Shim D-E and Hahn H T 2009 Intense pulsed light sintering of copper nanoink for printed electronics *Appl. Phys. A* **97** 791–8
- [25] Chung W-H, Hwang H-J and Kim H-S 2015 Flash light sintered copper precursor/nanoparticle pattern with high electrical conductivity and low porosity for printed electronics *Thin Solid Films* **580** 61–70
- [26] Park S-H, Chung W-H and Kim H-S 2014 Temperature changes of copper nanoparticle ink during flash light sintering *J. Mater. Process. Technol.* **214** 2730–8
- [27] Catala F 1999 From dicopper acetylide to carbyne *Polym. Int.* **48** 15–22
- [28] Garcia M A and Morse M D 2013 Electronic spectroscopy and electronic structure of copper acetylide, CuCCH *J. Phys. Chem. A* **117** 9860–70
- [29] Zhitnev Y N, Tveritinova E and Lunin V 2008 Catalytic properties of a copper-carbon system formed by explosive decomposition of copper acetylide *Russ. J. Phys. Chem. A* **82** 140–3
- [30] Sedoi V and Yavorovsky N 2008 Controlled synthesis of nanopowders via electrical explosion of wires *3rd Int. Forum on Strategic Technologies* pp 220–5
- [31] Wang Z, Fan A, Tian W, Wang Y and Li X 2006 Synthesis and structural features of Ni–Al nanoparticles by hydrogen plasma–metal reaction *Mater. Lett.* **60** 2227–31
- [32] Alqudami A, Annapoorni S and Shivaprasad S 2008 Ag–Au alloy nanoparticles prepared by electro-exploding wire technique *J. Nanopart. Res.* **10** 1027–36
- [33] Das R, Das B K and Shyam A 2012 Synthesis and characterization of copper nanoparticles by using the exploding wire method *J. Korean Phys. Soc.* **61** 710–2
- [34] Ryu J, Kim H-S and Hahn H T 2011 Reactive sintering of copper nanoparticles using intense pulsed light for printed electronics *J. Electron. Mater.* **40** 42–50
- [35] Chan G H, Zhao J, Hicks E M, Schatz G C and Van Duyne R P 2007 Plasmonic properties of copper nanoparticles fabricated by nanosphere lithography *Nano Lett.* **7** 1947–52
- [36] Zhai D, Zhang T, Guo J, Fang X and Wei J 2013 Water-based ultraviolet curable conductive inkjet ink containing silver nano-colloids for flexible electronics *Colloids Surf. A* **424** 1–9
- [37] Jiang H, Moon K-S and Wong C 2005 Synthesis of Ag–Cu alloy nanoparticles for lead-free interconnect materials *Proc. Int. Symp. on Advanced Packaging Materials: Processes, Properties and Interfaces* pp 173–7
- [38] Ceylan A, Jastrzebski K and Shah S I 2006 Enhanced solubility Ag–Cu nanoparticles and their thermal transport properties *Metall. Mater. Transactions A* **37** 2033–8
- [39] Niu Y, Gesmundo F, Viani F and Wu W 1997 The air oxidation of two-phase Cu–Ag alloys at 650 °C–750 °C *Oxid. Met.* **47** 21–52